

Multi-attribute seismic analysis – tackling non-linearity

Satinder Chopra[†], Doug Pruden⁺, Vladimir Alexeev[†]

AVO inversion for Lamé parameters ($\lambda\rho$ and $\mu\rho$) has become a common practice as it serves to enhance identification of reservoir zones. Also, integration of AVO-derived attribute volumes with other non-AVO derived seismic attribute volumes can provide meaningful geologic information when tied back to well data and verified as correlating with rock properties. Computation of reservoir properties for determination of mathematical relationships between variables derived from well logs, for example, is usually done with non-linear multivariate determinant analysis using neural networks. This paper provides a case study of a 3D seismic survey in southern Alberta, Canada, where a probabilistic neural network solution was first employed on AVO attributes (Pruden, 2002, Chopra & Pruden, 2003). Using the gamma-ray, acoustic and bulk density log curves over the zone of interest, gamma-ray and bulk density inversions were derived from the 3D attribute volumes. This methodology was successful, in that two new drilling locations derived from this work encountered a new gas charged reservoir, that not only extended the life of the gas pool but added new reserves as well.

Later, instead of neural networks, a different mathematical approach using cubic b-splines was utilized for the same purpose. The results were found to be similar, suggesting that apart from neural networks, the cubic b-splines could be used as a tool for tackling non-linearity in multi-attribute seismic analysis.

AVO inversion for Lamé parameters

The target area is a Lower Cretaceous glauconite filled fluvial channel, deposited within an incised valley system. A 3D seismic survey was acquired in order to create a stratigraphic model, consistent with all available well control and matching the production history. The ultimate goal was to locate undeveloped potential within the gas sands. The field has been producing since the early 1980s and two of the earliest, most prolific producers have begun to water out.

As the objective was stratigraphic in nature, the seismic data were processed with the objective of preserving relative amplitude relationships in the offset domain to allow for the use of AVO attribute analysis.

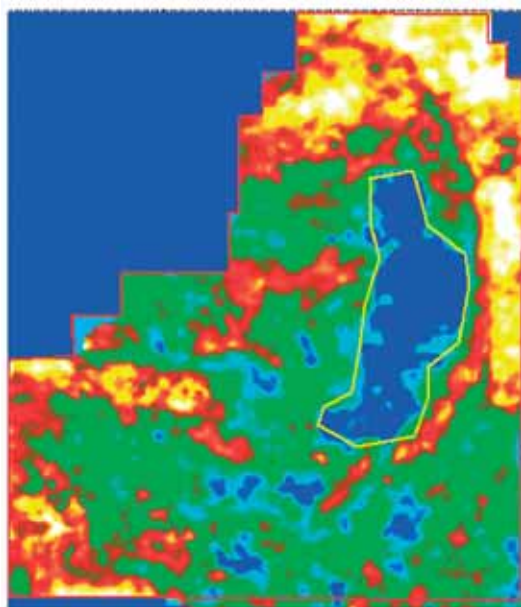


Fig 1a Time slice from Lambda-Rho showing the suspected gas anomaly. Low values of Lambda-Rho are shown in blue. The red polygon encloses all the live data points on both the time slices. The yellow polygon encloses the suspected anomaly.

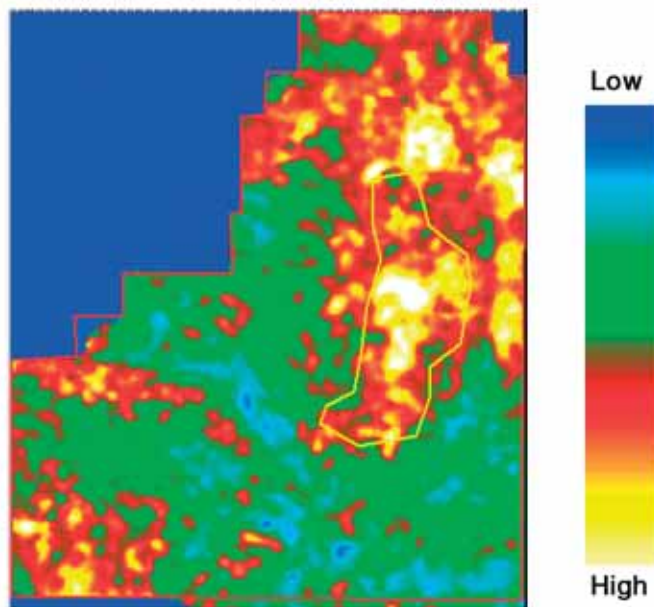


Fig 1b Time slice from Mu-Rho showing the suspected gas anomaly. High values of Mu-Rho are in yellow and red. The red polygon encloses all the live data points on both the time slices. The yellow polygon encloses the suspected anomaly.

[†]formerly at Core Lab Reservoir Technologies, Calgary

⁺formerly at GEDCO, Calgary, presently at Nose Creek Geophysical Inc., Calgary.

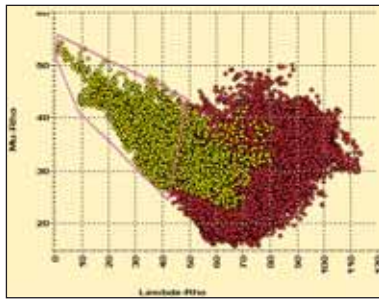


Fig 1c Cross-plot of Lambda-Rho vs Mu-Rho. The cross-plot shows the yellow points corresponding to low values of Lambda-Rho and high values of Mu-Rho which is expected of a gas anomaly. The purple polygon encloses the cluster points corresponding to the anomaly and lights up the anomaly in purple on the time slices (not shown).

Lithology and pore fluid information for the target subsurface formations can be studied in terms of the Lambda-Rho and Mu-Rho analysis (Goodway, 2001) where Lambda, Mu and Rho are the incompressibility, rigidity and density respectively. To do this first the P-wave and S-wave impedance reflectivity responses were estimated by solving the Fatti simplification of the Zoeppritz equations. The V_p/V_s ratio for the data was estimated from dipole sonic log data proximal to the area of study. Impedance reflectivities are related to Lamé parameters of incompressibility (λ) and rigidity (μ) by the relationships $\lambda\rho = I_p^2 - 2I_s^2$ and $\mu\rho = I_s^2$ where ρ is bulk density. The Lamé parameters cannot be directly extracted without an estimation of the density parameter ρ .

Figure 1 (a) and (b) shows the Lambda-Rho and Mu-Rho sections with the anomaly enclosed in a yellow polygon. The red polygon indicates all the live data points on the time slice that are brought into the Lambda-Rho vs Mu-Rho cross-plot space. The cross-plot for these two attributes is shown in Fig.1 (c) where yellow dots represent the values within the yellow polygons in figures 1 (a) and (b). In addition to gas sand identification, significant lithological information can be derived from the data.

Determination of non-linear relationships in well log parameters

The measured well log parameters like P-velocity, S-velocity, density, porosity and gamma ray are usually crossplotted to examine the cluster patterns for different lithologies. Depending on the shape of these clusters, linear or non-linear relationships can be determined for the pair of attributes crossplotted, and then used in the transformation of seismic attributes into desired reservoir parameters. Sometimes, the shapes of the clusters or the scatter of the individual points on the crossplot make it difficult to determine a mathematical relationship in terms of its accuracy. Examples of this are the determination of a linear fit to an almost circular spread of points or a non-linear fit to an irregular shaped cluster.

Given that the gamma ray logs in this area are diagnostic of sands, gamma ray logs exist for each well and there is a fairly even sampling of well data across the field, a deterministic approach was found that allowed us to quantitatively relate the measured seismic attributes to the gamma ray data. A simple analysis of the relationship of gamma ray values to acoustic impedance suggested that while a general relationship between the two is visually apparent, it is clearly a non-linear relationship. Further analysis of the other attributes with the gamma ray curve produced similar results.

Using neural networks

A non-linear multi-variate determinant analysis between the derived multiple seismic attribute volumes and the measured gamma ray values at wells is a problem that is ideally suited for neural networks. By training a neural network with a statistically representative population of the targeted log responses and the multiple seismic attribute volumes available at each well, a non-linear multi-attribute transform can be computed to produce an inversion volume of the targeted log type (Hampson et al, 2001, Leiphart and Hart, 2001).

Using the gamma ray, acoustic and bulk density log curves available over the zone of interest for the 16 wells, the neural network procedure was employed to derive gamma ray and bulk density inversions across the 3D volume. The resulting gamma ray inversion is shown on the horizon slice in Figures 2 (the same slice as shown previously). The data are scaled to API gamma units in Figure 2 and converted to porosity in Figure 3 using the following standard linear density relationship.

$$\rho_b = \phi\rho_f + (1-\phi)\rho_{ma}$$

where ρ_b = bulk density

ϕ = porosity

ρ_{ma} = a clean formation of known matrix density

ρ_f = a fluid of average density

From log data, the sand filled channels are interpreted as having gamma values less than 50 API gamma units. This cut-off value was used to mask out inverted density values for silts and shales. Analysis of Figures 2a and 2b shows three distinct sand bearing channels.

Using cubic b-splines

Spline curves (or mathematical representation of the approximating curves in the form of polynomials) have been used with a certain degree of accuracy depending on trade-offs between drawing complexity and the generality of the curve space that they exhibit. Instead of letting the spline pass through each of the cluster points, it is possible to specify control points on the cross-plot, based on the premise that the human eye can be relied upon to determine the desired shape of the approximating spline. B-splines are approximating spline curves with the advantage that the degree of

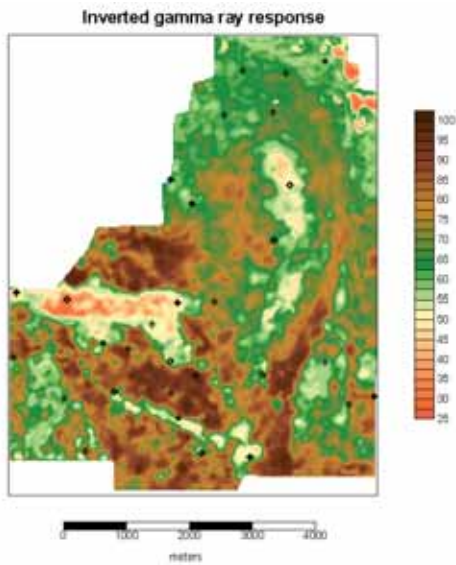


Figure 2 Neural network inverted gamma ray response. Note the distinct separation of sand from silt and shale.

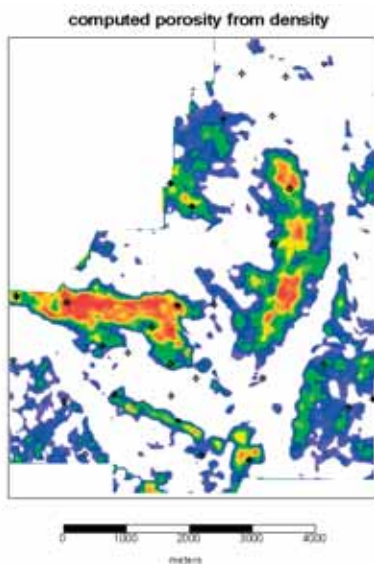


Figure 3 Neural network computed porosity from inverted density response. The density values have been masked out for gamma ray values representative of silt or shale, giving a relative porosity indicator for the sands.

polynomial is independent of the number of points and its shape is controlled locally in that adjusting a single point does not require total reconstruction of the curve. Of course the added computation complexity may be taken as a disadvantage. In our computation we assume that the given data are samples of a polynomial function of two variables with the samples randomly distributed in the function's domain and there is no known connectivity between the samples. A set of control points is marked on the cluster and cubic b-splines are used with a minimum of four nearest points, then shifted by one sample at a time and finally concatenating the

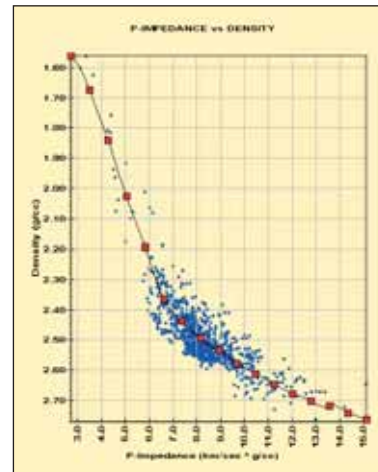


Figure 4 Crossplot of P-impedance versus density. Control points for the spline function are in red.

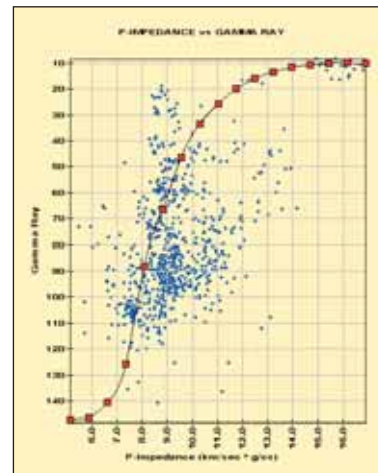


Figure 5 Crossplot of P-impedance versus gamma ray

multiple 4-point splines.

The choice of the splines's control points needs to be done carefully in that the curve through them should achieve a faithful representation of the data.

Figure 4 depicts a cross-plot of P-impedance versus density for a well falling within a 3D seismic volume of the case study discussed above.

A cubic b-spline curve is seen overlaid on the cluster passing through the control points (in red) marked as a guide for the best fit curve.

The crossplot for P-impedance versus gamma ray for a broad zone covering the desired sand zone shows a scatter of points as shown in Figure 5. While the upper (<70) values can be seen to be representative of the sandstone, the lower (>70 values) represent the silt and shale. Consequently, the control points were marked to go through the sandstone cluster. Similarly, a reasonable fit was obtained for P-impedance versus porosity.

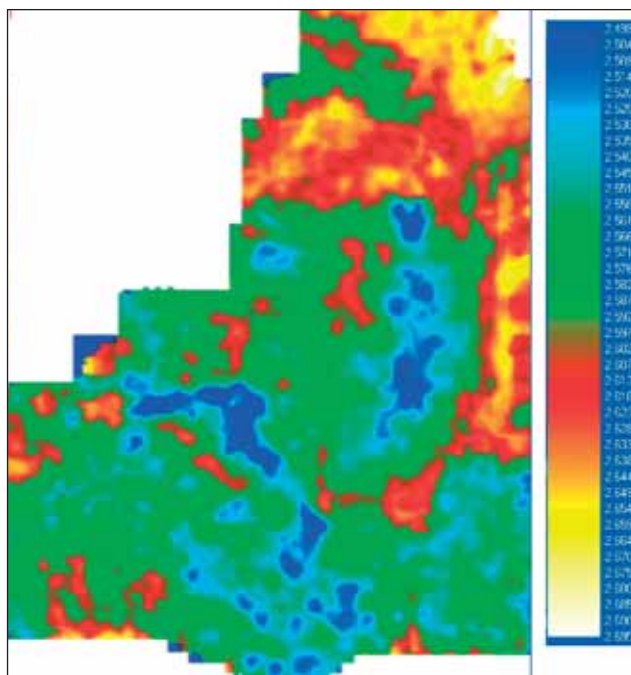


Figure 6 Spline curve inverted density. The time slice is referenced to Figure 1.

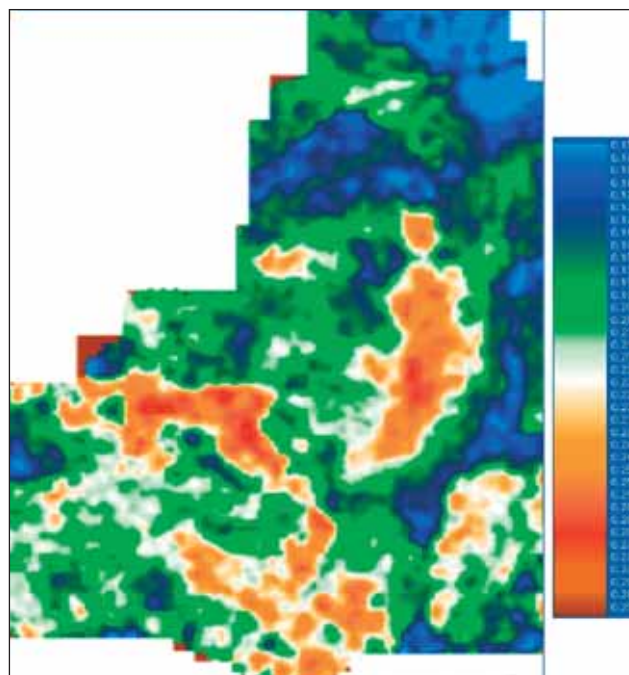


Figure 8 Spline curve inverted porosity. The time slice is referenced to Figure 1.

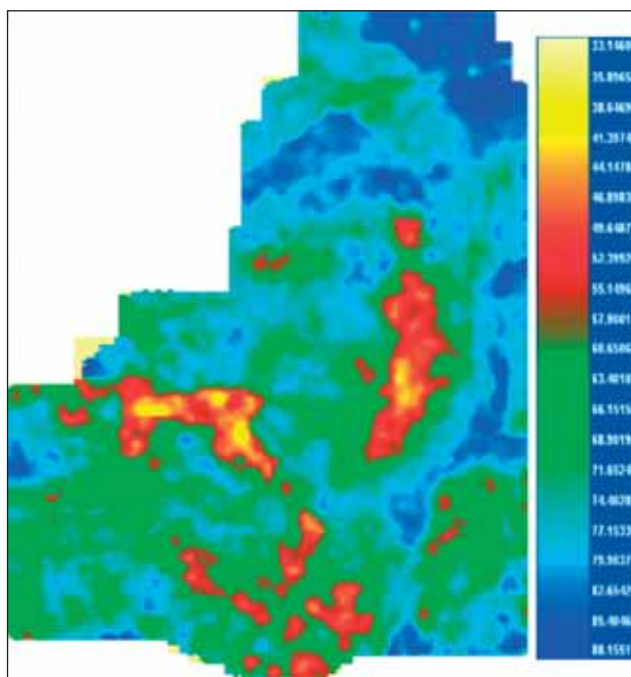


Figure 7 Spline curve inverted gamma ray. The time slice is referenced to Figure 1.

The determined mathematical relationships (polynomial) for these curves was used to transform the acoustic impedance inversion volume to density (Figure 6), gamma ray (Figure 7) and porosity (Figure 8) volumes. Time slices as referenced to Figure 1 were displayed for each of the volumes.

Notice the close similarity between the gamma ray (Figure 7) and porosity (Figure 8) anomalous patterns corresponding to the sands. The results are encouraging especially as the mathematical relationships determined from one well has yielded results that are similar to a neural network approach followed earlier.

Integrating multi-attribute volumes

Application of AVO inversion to a 3D seismic volume yields several attribute volumes that contain fluid and lithological information. It is quite overwhelming for a seismic interpreter to churn through many attribute volumes and draw his conclusions. The usual practice entails displaying each attribute volume and looking for anomalous zones and confirm their consistency in the different volumes. For example, a prospective gas sand will show up low values of Lambda-Rho, high values of Mu-Rho, low values of density, high values of porosity and a suitable range of values of gamma ray.

An automated procedure was developed wherein all the five input volumes could be read in and a desired range of values specified corresponding to the gas anomalies. Figure 9 shows a time slice as referenced to Figure 1. Notice the gas sand distribution matches that show up on the individual slices in Figures 2 and 3 and 6, 7 and 8. Alternatively, another composite volume has been generated employing a mathematical operation that optimizes the display of the anomalous zone e.g. an operation of the form $(\text{Lambda}/\text{Mu}) * (\text{gamma ray}/\text{porosity}) * \text{density}$. A time slice from this volume is shown in Figure 10, wherein one sees the expected pattern for prospective gas sands.

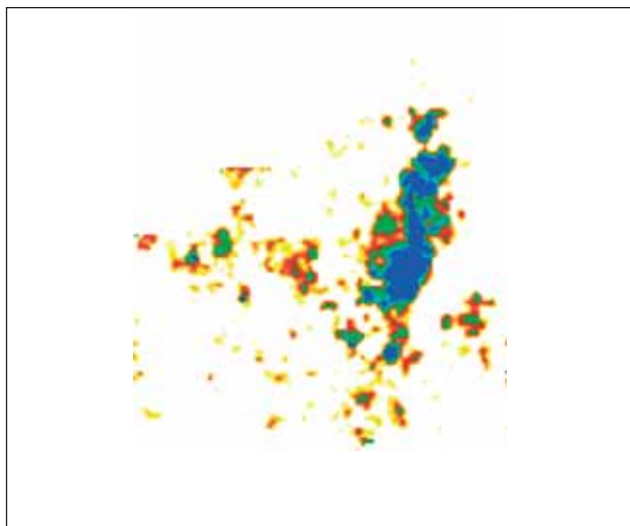


Figure 9 Time slice from composite volume with a restricted range of values for the individual attributes. The time slice is referenced to Figure 1.

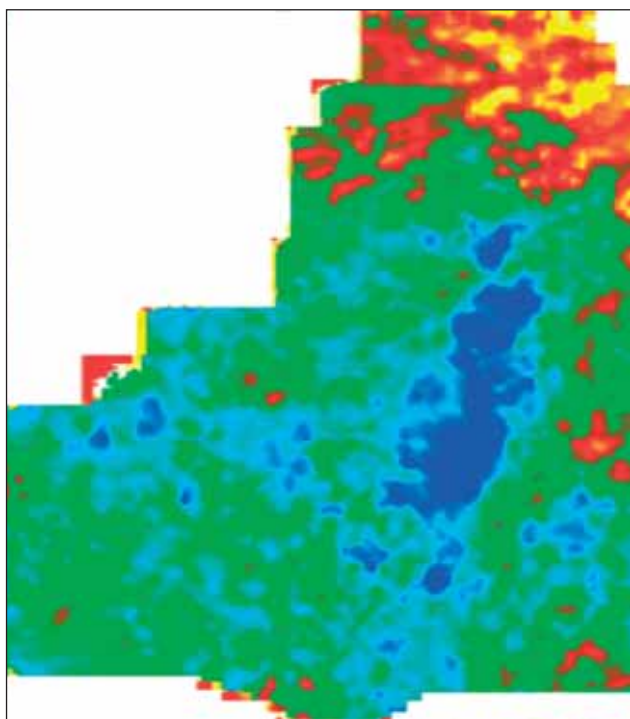


Figure 10 Time slice from composite volume optimizing the anomalous zones. The time slice is referenced to Figure 1.

Conclusions

1. Integration of AVO inversion in terms of Lamé parameters was done with seismic attributes volumes derived using cubic b-spline analysis on well log data. The results were found to be similar to an analogous integration done using neural network analysis.
2. The derived volumes, i.e. gamma ray, density and porosity contribute to the estimation of relative sand distribution and fluid content estimates.
3. A composite volume for integrating different AVO attribute volumes have been generated that show convincing results. Use of such volumes can save seismic interpreters the drudgery of looking through individual attribute volumes.

While the above exercise has yielded convincing results, it needs to be mentioned that the results depend on the choice of clusters (e.g. gamma ray) used for the determination of the mathematical relationships. Besides, the question of whether the given well is representative of the geological space under consideration will need an affirmative answer. This approach could be difficult in areas that have a significant variability in geology in a lateral sense.

References

- Chopra, S. and Pruden, D. [2003] Multi-Attribute Seismic Analysis on AVO derived parameters – a case study. *The Leading Edge*, SEG Publication, 2003.
- Goodway, W.N. [2003] AVO and Lamé constants for rock parameterization and fluid detection. *CSEG Recorder*, 26, 6, 39-60.
- Hampson, D.P., Schuelke, J.S., and Querien, J.A. [2001] Use of multiattribute transforms to predict log properties from seismic data. *Geophysics*, 66, 220-236.
- Leiphart, D.J. and Hart, B.S. [2001] Comparison of linear regression and a probabilistic neural network to predict porosity from 3-D seismic attributes in Lower Brushy Canyon channeled sandstones, southeast New Mexico. *Geophysics*, 66, 1349-1358.
- Pruden, D. M. [2002] Extracting meaningful geologic parameters using multiple attribute analysis on AVO derived Lamé rock parameter inversions: 3D seismic case study from southern Alberta, Canada. *Expanded abstracts, 72nd Ann. Mtg. Soc. Expl. Geophys.*